2004

Investigation of forward and reverse current conduction in GaN films by conductive atomic force microscopy

J. Spradlin
Virginia Commonwealth University

S. Doğan
Virginia Commonwealth University

J. Xie
Virginia Commonwealth University, xiej@vcu.edu

See next page for additional authors

Spradlin. J., Doğan, S., Xie, J., et al. Investigation of forward and reverse current conduction in GaN films by conductive atomic force microscopy. Applied Physics Letters, 84, 4150 (2004). Copyright © 2004 AIP Publishing LLC.

Investigation of forward and reverse current conduction in GaN films by conductive atomic force microscopy

J. Spradlin, S. Doğan,[a] J. Xie, R. Molnar,[b] A. A. Baski,[c] and H. Morkoç
Department of Electrical Engineering and Department of Physics, Virginia Commonwealth University, Richmond, Virginia 23284

(Received 16 October 2003; accepted 22 March 2004; published online 6 May 2004)

We have used conductive atomic force microscopy (C–AFM) to investigate the forward and reverse bias current conduction of homo- and heteroepitaxial GaN-based films grown by molecular beam epitaxy. In the case of homoepitaxy, C–AFM shows enhanced current conduction at the centers of ~30% of spiral hillocks, which are associated with screw dislocations. Local current–voltage spectra taken by C–AFM on and off such hillocks indicate Frenkel–Poole and field emission mechanisms, respectively, for low current levels in forward conduction. In the case of heteroepitaxial GaN films grown on sapphire, the correlation between conduction pathways and topography is more complex. We do observe, however, that films with more rectifying nominal Schottky behavior (less reverse leakage current) produce forward and reverse bias C–AFM images with strong asymmetry. © *2004 American Institute of Physics.* [DOI: 10.1063/1.1751609]

Anomalies in current conduction can limit the performance of electronic devices, and GaN is no exception. The source of anomalies such as excess current has been in debate; however, point defects undoubtedly play a role. Such defects can form complexes with extended defects, and show selective uptake of impurities such as oxygen. Some groups attribute abnormal electrical characteristics to surface states,[1–3] while others cite dislocations[4–6] or bulk defects.[7–9] The local electrical properties of films can be directly probed using conductive atomic force microscopy (C–AFM), where a metallized tip acts as a microscopic Schottky contact. Simultaneous images of the surface topography and tip-sample current can lead to the identification of features associated with enhanced current conduction. Previous groups[10–12] have used C–AFM to show that screw dislocations are correlated with reverse bias current leakage. Incorporation of excess Ga at screw dislocations has been proposed as a mechanism.[11,13] In addition, oxygen related impurity accumulation near open cores[14] could be responsible for increased current leakage. In this work, we confirm this leakage behavior and show local Schottky barrier current–voltage curves on and off a defective site, both in forward and reverse bias, and identify the conduction mechanism. In addition, we examine the conduction behavior in both forward and reverse bias for heteroepitaxial films with significantly different Schottky behavior.

The samples used in this investigation include an AlGaN/GaN film grown on a hydride vapor phase epitaxy (HVPE) GaN template (sample A), and two GaN films grown on sapphire substrates (samples B and C). All films were grown using molecular beam epitaxy (MBE) under Ga-rich conditions with radio-frequency plasma nitrogen (sample A) or ammonia (samples B and C) as the nitrogen source. Sample A is a 20-nm-thick $Al_{0.12}Ga_{0.88}N$ layer on a 1 μm GaN buffer, and samples B and C are ~2.5-μm-thick Ga-polar GaN films. Sample B was grown at a lower temperature (880 °C) with a lower III/V ratio as compared to sample C (925 °C), and represents a higher-quality reference sample with $n=10^{17}$ cm^{-3} at RT.[15] $I-V$ measurements of Schottky diodes were obtained on samples B and C using a Keithley 4200 SCS parameter analyzer. Curve fitting of the $I-V$ data was based on a function used in Suzue *et al.*,[16] where two tuning parameters (slope and intercept) were chosen for conduction mechanisms.[17,18] For C–AFM measurements, ohmic contacts were formed on all samples using Ti/Al/Ti/Au metallization and the tip formed a microscopic Schottky contact. The data were acquired using a Dimension 3100 atomic force microscope (AFM) with Pt-coated cantilevers and either a C–AFM (200 pA–2 μA) or tunneling amplifier (1–100 pA) module. In this letter, current images are presented such that brighter regions always indicate higher current conduction.

The AFM topography and C–AFM current images for sample A are shown in Fig. 1, where the surface consists of pyramidal hillocks that are 150–500 nm wide and have a density of $\sim 5\times10^{8}$ cm^{-2}. The C–AFM images for reverse and forward bias conditions are shown below the topography images. Enhanced current conduction occurs in both forward and reverse biases at the centers of the pyramidal hillocks, which are likely associated with screw dislocations. Approximately 30% of these features conduct at the maximum reverse bias of 12 V. The number of features demonstrating conduction increases with increasing bias. Note that the larger circles superimposed in Figs. 1(b) and 1(c) indicate hillocks that conduct at both biases, where the extent of such conduction is significantly larger in forward bias. The smaller circles indicate conduction centers in reverse bias that are not prevalent in forward bias. Therefore, only a fraction of the hillocks appear to be amphoteric.

Using C–AFM, localized $I-V$ spectra were taken from

[a]Also at: Atatürk University, Department of Physics, 25240 Erzurum, Turkey.
[b]Present address: Massachusetts Institute of Technology, Lincoln Laboratory.
[c]Author to whom correspondence should be addressed; electronic mail: aabaski@vcu.edu

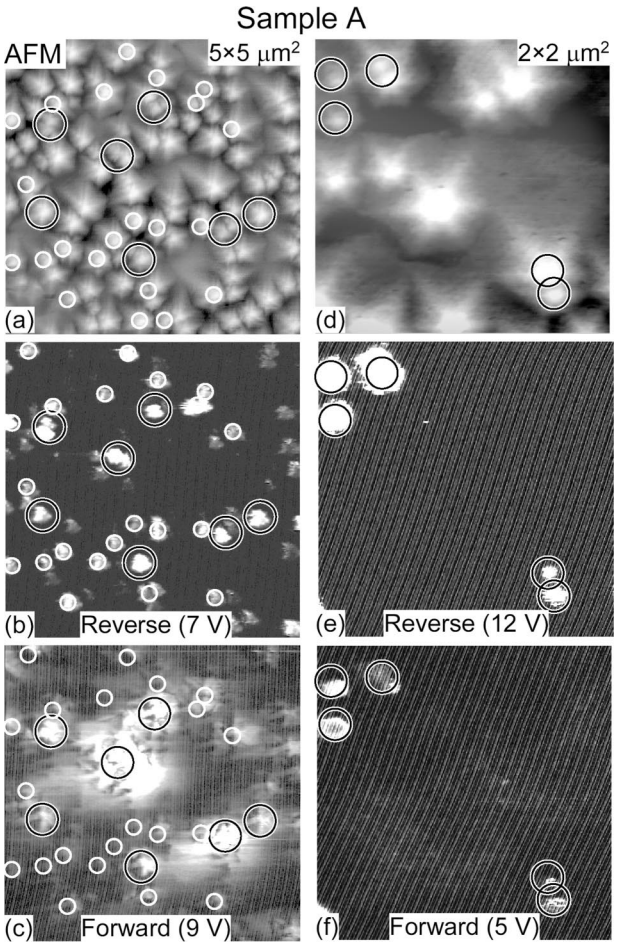

FIG. 1. AFM and C–AFM images of sample A, which is a modulation-doped field effect transistor structure grown on a HVPE template. (a) $5\times5\ \mu m^2$ image of topography ($\Delta z = 25$ nm) and (b), (c) simultaneous C–AFM current images for reverse and forward bias ($\Delta z = 200$ pA), respectively. (d) $2\times2\ \mu m^2$ topography and (e), (f) simultaneous C–AFM for reverse and forward bias ($\Delta z = 10$ pA), respectively. White/black circles indicate current leakage centers.

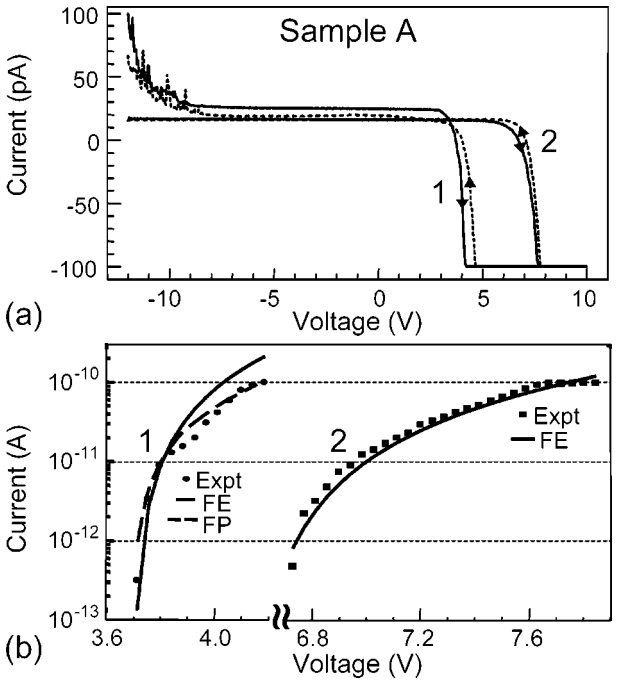

FIG. 2. (a) Local I–V spectra taken using C–AFM on sample A for curve 1 on a hillock and curve 2 off a hillock. The spectra were acquired using a current amplifier which limits the maximum current to 100 pA, and with negative voltages corresponding to reverse bias conditions. (b) Fitting of current conduction mechanisms to the forward bias data of curves 1 and 2, where FE = field emission and FP = Frenkel–Poole.

regions located both on and off the hillocks, as seen in Fig. 2(a). Curve 1 on a hillock shows detectable leakage in reverse bias at ~9 V, whereas region 2 off a hillock shows no measurable leakage. The forward turn-on voltage is also seen to shift down to ~3 V on a hillock versus ~8 V in defect-free regions. These turn-on voltages have some variation across the sample, e.g., Fig. 1(c) indicates that defect-free areas become conductive at voltages slightly higher than 9 V. Note that the relatively high turn-on voltages observed for C–AFM indicate a significant voltage drop outside the tip-semiconductor junction. The observed shifts in forward and reverse bias for current conduction on the hillock indicate the possibility of charge trapping effects. Subsequent $I-V$ spectra at the same location show a significant decrease in current after three to five scans, also indicating such charging effects. Fitting of the observed forward current data to various current conduction mechanisms, as shown in Fig. 2(b), indicates that current conduction is consistent with Frenkel–Poole in the defective hillock region, and field emission current away from the defect. $I-V$ data obtained from macroscopic (standard) Schottky contacts indicate that thermionic field emission is the primary mechanism at higher current levels in forward bias.

In addition to layers grown on HVPE templates, we have also examined MBE samples grown directly on sapphire. Figure 3 shows C–AFM results for sample B [Figs. 3(a)–3(c)] and sample C [Figs. 3(d)–3(f)], which were found to produce higher and lower quality standard Schottky contacts, respectively. The topography of sample B shows a high density of islands having a uniform size of ~150 nm. The C–AFM current images indicate only a few isolated leakage paths at a reverse bias of 12 V. Under forward bias conditions, we observed enhanced current along the perimeters of islands and found that conducting areas increased in area with increasing voltage. Figure 3(c) shows significant conduction at 4 V bias, where small black regions indicate non-conducting regions at the centers of islands. The topography of sample C is significantly rougher and shows a high density of leakage centers at only 4 V reverse bias, where such leakage does not strongly correlate with sample topography. In forward bias, a comparable density of conductive regions occurs. Sample C therefore demonstrates uniform current conduction at localized areas for both biases, whereas sample B displays few leakage centers at reverse bias and significant current conduction at increased forward bias.

To correlate the local conduction behavior observed by C–AFM with macroscopic behavior, Schottky contact $I-V$ characteristics were also examined. Figure 4 shows the $I-V$ curves of samples B and C, where sample B is higher quality with better rectifying behavior and lower leakage current. The C–AFM data are consistent with these $I-V$ curves, showing qualitatively different images in forward and reverse bias for sample B, and similar images at opposite bias for sample C. Our fitting of the $I-V$ data for sample B indicates a field emission mechanism at low forward bias (<1

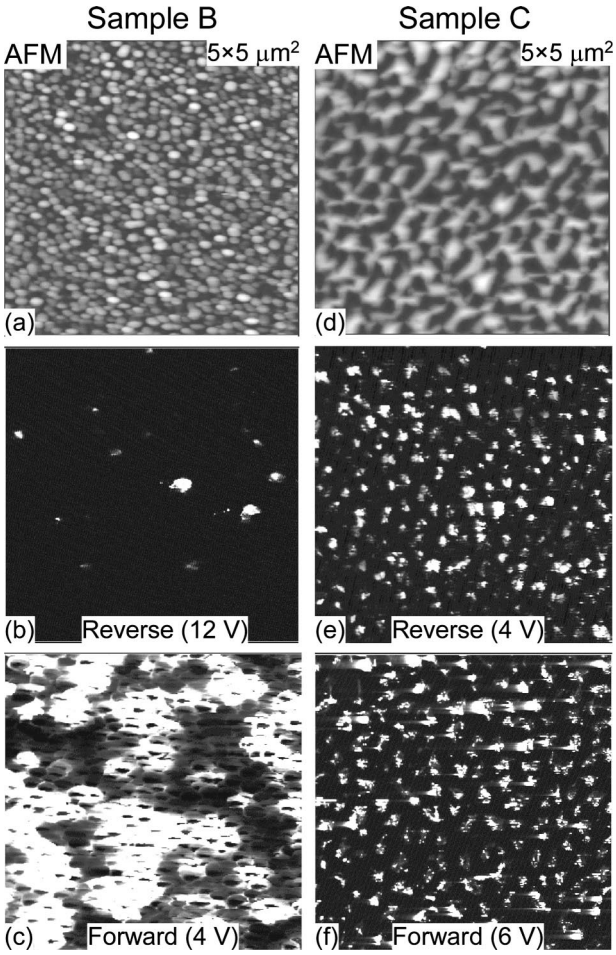

FIG. 3. AFM and C–AFM images of samples B and C, which are MBE heteroepitaxial layers grown on sapphire. All images are $5\times5\ \mu m^2$ and C–AFM images are not correlated to topography. (a) Sample B topography ($\Delta z = 35$ nm) and (b), (c) C–AFM current images for reverse bias ($\Delta z = 2$ pA) and forward bias ($\Delta z = 100$ pA), respectively. (d) Sample C topography ($\Delta z = 175$ nm) and (e), (f) C–AFM images for reverse and forward bias ($\Delta z = 200$ pA), respectively.

V), thermionic field emission at high forward bias, and a hopping mechanism at reverse bias. Sample C is best fit using a Frenkel–Poole mechanism for both reverse and forward bias, which is indicative of poor sample quality.[17] This behavior is consistent with the C–AFM $I-V$ data of defective areas on sample A, which also show Frenkel–Poole conduction in forward bias.

In summary, C–AFM data for both reverse and forward bias conditions have been shown for MBE-grown, GaN-based samples on a HVPE template, as well as directly on a sapphire substrate. For the film on a HVPE template, we observe premature current breakdown at the centers of hillocks associated with screw dislocations, consistent with the results of other groups. Local $I-V$ curves of such dislocations are presented which indicate a Frenkel–Poole mechanism for forward conduction on defective regions, as opposed to field emission on nondefective regions. For the films grown directly on sapphire, C–AFM data do not show a straightforward correlation between topography and current conduction. It is found, however, that more rectifying Schottky behavior with small reverse current is correlated with significant asymmetry in forward and reverse bias C–AFM images.

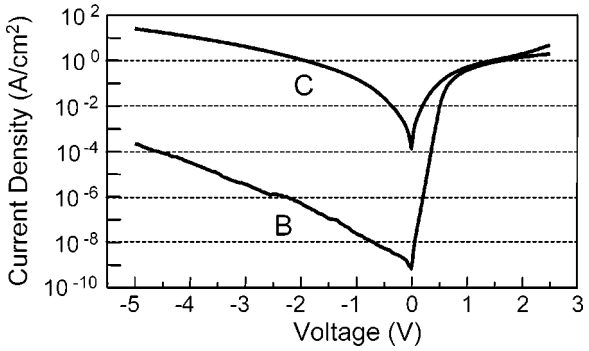

FIG. 4. I–V spectra taken on samples B and C using 75 μm diameter, Ni/Au Schottky contacts. Sample B indicates a field emission or thermionic field emission mechanism for forward bias, and a hopping mechanism at reverse bias. Sample C is best fit using a Frenkel–Poole mechanism for both reverse and forward bias.

This research was funded by grants from the National Science Foundation (Dr. V. Hess) and Air Force Office of Scientific Research (Dr. G. L. Witt).

[1] D. C. Look and Z.-Q. Fang, Appl. Phys. Lett. **79**, 84 (2001).
[2] A. Rizzi, Appl. Surf. Sci. **190**, 311 (2002).
[3] W. Liu, M. F. Li, S. J. Chua, N. Akutsu, and K. Matsumoto, Semicond. Sci. Technol. **14**, 399 (1999).
[4] J. W. P. Hsu, M. J. Manfra, D. V. Lang, S. Richter, S. N. G. Chu, A. M. Sergent, R. N. Kleiman, L. N. Pfeiffer, and R. J. Molnar, Appl. Phys. Lett. **78**, 1685 (2001).
[5] K. Shiojima, J. M. Woodall, C. J. Eiting, P. A. Grudowski, and R. D. Dupuis, J. Vac. Sci. Technol. B **17**, 2030 (1999).
[6] E. G. Brazel, M. A. Chin, and V. Narayanamurti, Appl. Phys. Lett. **74**, 2367 (1999).
[7] C. B. Soh, D. Z. Chi, A. Ramam, H. F. Lim, and S. J. Chua, Mater. Sci. Semicond. Process. **4**, 595 (2001).
[8] P. Muret, A. Philippe, E. Monroy, E. Munoz, B. Beaumont, F. Omnes, and P. Gibart, J. Appl. Phys. **91**, 2998 (2002).
[9] A. Hierro, D. Kwon, S. A. Ringel, M. Hansen, J. S. Speck, U. K. Mishra, and S. P. DenBarrs, Appl. Phys. Lett. **76**, 3064 (2000).
[10] B. S. Simpkins, E. T. Yu, P. Waltereit, and J. S. Speck, J. Appl. Phys. **94**, 1448 (2003).
[11] J. W. P. Hsu, M. J. Manfra, R. J. Molnar, B. Heying, and J. S. Speck, Appl. Phys. Lett. **81**, 79 (2002).
[12] K. Shiojima and T. Suemitsu, J. Vac. Sci. Technol. B **21**, 698 (2003).
[13] J. E. Northrup, Appl. Phys. Lett. **78**, 2288 (2001).
[14] I. Arslan, S. Ogut, P. D. Nellist, and N. D. Browning, Proc. of the 4th Symp. on NonStoichiometric III–V Compounds, 2002, Vol. 27, p. 145.
[15] J. Spradlin, S. Doğan, M. Mikkelson, D. Huang, L. He, D. Johnstone, H. Morkoç, and R. J. Molnar, Appl. Phys. Lett. **82**, 3556 (2003).
[16] K. Suzue, S. N. Mohammad, Z. F. Fan, W. Kim, O. Aktas, A. E. Botchkarev, and H. Morkoç, J. Appl. Phys. **80**, 4467 (1996).
[17] See, for example, H. Morkoç, *Nitride Semiconductors and Devices* (Springer, Berlin, 1999), for details and nomenclature with regard to current conduction mechanisms.
[18] H. Hasegawa and S. Oyama, J. Vac. Sci. Technol. B **20**, 1647 (2002).